Reducing losses and dispersion effects in multilayer metamaterial tunnelling devices

2005 New J. Phys. 7 166

(http://iopscience.iop.org/1367-2630/7/1/166)

New Journal of Physics
The open-access journal for physics

Reducing losses and dispersion effects in multilayer metamaterial tunnelling devices

Juan D Baena[1], Lukas Jelinek[2] and Ricardo Marqués[1]

[1] Department of Electronics and Electromagnetism, Faculty of Physics, University of Seville, Avenida Reina Mercedes, 41012 Seville, Spain
[2] Department of Electromagnetic Field, Czech Technical University, Technicka 2, 16627-Prague 6, Czech Republic
E-mail: juan_dbd@us.es, jelinel1@fel.cvut.cz and marques@us.es

New Journal of Physics **7** (2005) 166
Received 1 April 2005
Published 8 August 2005
Online at http://www.njp.org/
doi:10.1088/1367-2630/7/1/166

Abstract. This paper focuses on reduction of losses and dispersion effects on tunnelling through waveguides filled with metamaterial. It will be shown that these unwanted effects could be reduced by dividing the metamaterial into several regions separated by air slabs. In the first part, these effects will be studied for isotropic left-handed media (LHM). Later this will be substituted by an anisotropic magnetic medium which will lead to a practical realization with broadside coupled split ring resonators (BC-SRRs). Finally, it is shown that quasi-perfect tunnelling is possible, even in the presence of unavoidable losses and dispersion in the metamaterial.

Contents

PII: S1367-2630(05)97357-6

1. Introduction

Left-handed media (LHM) were introduced by Veselago [1] as materials with simultaneous negative permittivity and permeability. However, no such materials have been found in Nature. In 1999, Pendry *et al* [2] proposed the split ring resonator (SRR) as a basic constituent of artificial negative permeability media. After this seminal work, Smith *et al* [3] manufactured the first artificial LHM by superposing SRRs and metallic wires which provide negative permittivity. Later, Shelby *et al* [4] demonstrated experimentally negative refraction, previously predicted by Veselago. Veselago's analysis of the focusing properties of LHM was continued by Pendry [5], who showed that a left-handed slab of $\varepsilon/\varepsilon_0 = \mu/\mu_0 = -1$ will act as a 'perfect lens' producing perfect sub-wavelength imaging. This behaviour was explained by means of amplification of evanescent waves inside the left-handed slab. This idea was experimentally demonstrated by Grbic and Eleftheriades [6] in an analogous planar microwave circuit and by Lagarkov and Kissel [7] in an anisotropic planar slab. Amplification and tunnelling of evanescent waves have been also experimentally demonstrated in a rectangular waveguide loaded with a left-handed slab [8]. Since the fundamental electromagnetic mode in a rectangular waveguide is the superposition of two symmetrical plane waves [9], those results can be directly applied to the study of amplification and tunnelling of plane waves in left-handed slabs surrounded by free space. In addition, since isolated evanescent modes can be easily excited in a waveguide, a considerable simplification of the analysis is obtained.

There are some practical limitations for obtaining sub-wavelength resolution using a left-handed slab. It was shown in [10]–[12] that losses and dispersion affect the resolution dramatically. Reduction of losses and dispersion effects in these devices is thus a key issue from a practical standpoint. In 2001, Shamonina *et al* [13] suggested to use a distributed metamaterial (or multilayered metamaterial) in order to reduce these unwanted effects. A practical realization of this idea at optical frequencies was proposed by other authors [14, 15]: a layered stack of thin dielectric and metal slices. However, to the best of our knowledge, this idea has not yet been applied to a system made of SRRs which allows us to design devices in a wide range of frequencies. The main aim of this paper is to study the usefulness of multilayered metamaterial structures for enhancing the tunnelling of power in the waveguide configuration analysed in [8]. Firstly, a systematic analysis of losses and dispersion effects on the tunnelling through the waveguide filled with a multilayer stack of isotropic LHM and vacuum slices will be considered. A clear connection with the sub-wavelength focusing by a LHM slab will be highlighted. Secondly, the isotropic LHM will be substituted by an anisotropic magnetic medium obtaining a similar behaviour. Finally a practical realization of this last idea using broadside coupled split ring resonators (BC-SRRs) [16] will be proposed and analysed through numerical simulations.

2. Analysis of perfect tunnelling

An example of a structure exhibiting tunnelling effect is shown in figure 1(a). The figure shows a hollow waveguide section below cutoff ($a < \lambda_0/2$), sandwiched between two semi-infinite propagative waveguides with the same transversal dimensions. Input and output sections are filled with dielectric of permittivity higher than ε_0 to allow energy propagation. Transmission through the middle section decreases when its length increases, due to the exponential decay of the electromagnetic field in the 'in cutoff' waveguide section. To calculate the transmission

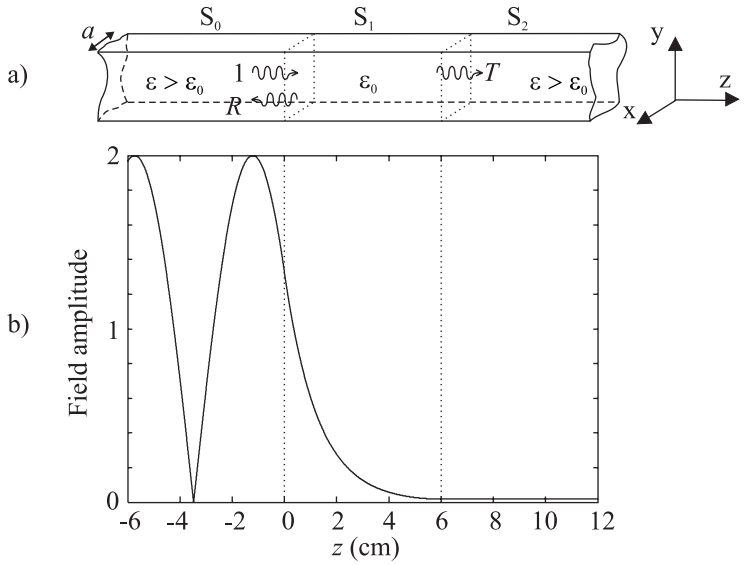

Figure 1. (a) Conventional waveguide tunnelling structure. (b) Field amplitude along the structure. The permittivity of input (S_0) and output (S_2) waveguide is $\varepsilon/\varepsilon_0 = 2$.

shown in figure 1(b), the incident wave is assumed to be the fundamental mode TE_{10}, and typical boundary conditions at transitions have been imposed. Note that no other modes are excited at the transitions, since all sections have the same transversal dimensions. Therefore, the field distribution within each section is described by:

$$\begin{aligned} \mathbf{E} &= E_y^0 \sin(\pi x/a) \exp(\pm \mathrm{i} k_z z)\hat{\mathbf{y}}, \\ \mathbf{H} &= (H_x^0 \sin(\pi x/a)\hat{\mathbf{x}} + H_z^0 \cos(\pi x/a)\hat{\mathbf{z}}) \exp(\pm \mathrm{i} k_z z), \end{aligned} \tag{1}$$

where the propagation wave number is

$$k_z = \sqrt{(\omega/c_0)^2 \varepsilon_r \mu_r - (\pi/a)^2}. \tag{2}$$

It is apparent from figure 1(b) that transmission in this device is very low. However, it was shown in [8] that it can be substantially enhanced by filling the waveguide with LHM as in figure 2(b). In that paper it was also shown that losses and dispersion forbid complete transmission. However, quasi-perfect tunnelling can be achieved when they are small.

In order to reduce the effect of losses, multilayer metamaterial configurations (see figure 2) will be analysed. As in the previous example, the fundamental mode will also be considered here. The transmission and reflection coefficients, T and R, of these devices can be easily obtained by cascading the transmission matrices of discontinuity interfaces, $\mathbf{Z}_{ij}$, and propagation through the sections, $\mathbf{T}_i$, as was done in [9]:

$$\begin{pmatrix} 1 \\ R \end{pmatrix} = \mathbf{Z_{0,1}} \cdot \mathbf{T_1} \cdot \mathbf{Z_{1,2}} \cdot \mathbf{T}_2 \cdot \cdots \cdot \mathbf{T}_N \cdot \mathbf{Z}_{N,N+1} \cdot \begin{pmatrix} T \\ 0 \end{pmatrix}, \tag{3}$$

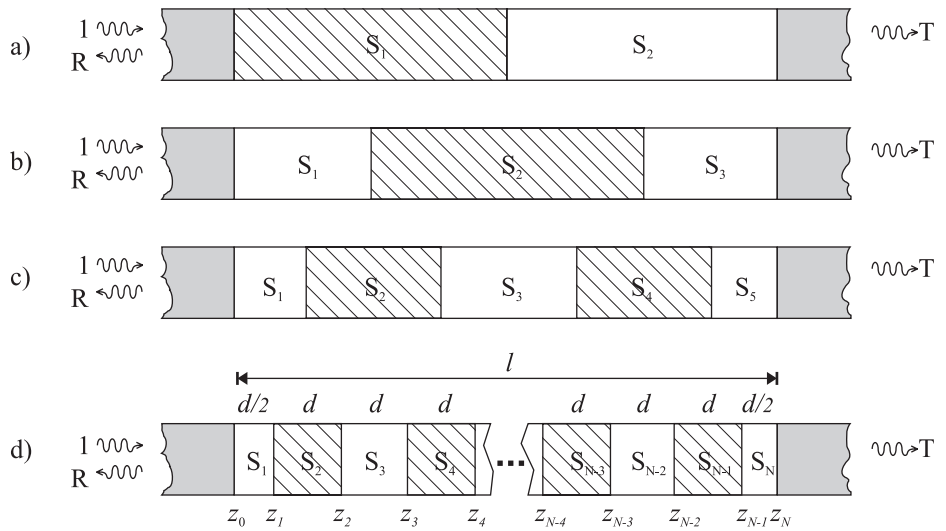

Figure 2. Waveguide structures for different numbers of metamaterial regions. The values of permittivity and permeability are: $\varepsilon/\varepsilon_0 = 2$, $\mu/\mu_0 = 1$ (grey); $\varepsilon/\varepsilon_0 = \mu/\mu_0 = 1$ (white); $\varepsilon/\varepsilon_0 = \mu/\mu_0 = -1$ (striped). The figure shows the zeroth-, first-, second- and mth-order structures, where m is the number of vacuum–metamaterial interfaces. The number of inner regions is $N = 2^m + 1$.

where

$$\mathbf{Z}_{i,j} = \frac{1}{2Z_j}\begin{pmatrix} Z_j + Z_i & Z_j - Z_i \\ Z_j - Z_i & Z_j + Z_i \end{pmatrix}, \tag{4}$$

$$\mathbf{T}_i = \begin{pmatrix} \exp(\alpha_i l_i) & 0 \\ 0 & \exp(-\alpha_i l_i) \end{pmatrix}, \tag{5}$$

where Z_i is the impedance and α_i the attenuation constant of the fundamental mode in the ith section. In figure 2, the striped regions represent waveguide sections filled with left-handed material of $\mu/\mu_0 = \varepsilon/\varepsilon_0 = -1$, whereas the white regions stand for empty waveguide sections. These sections are sandwiched between two propagative waveguides filled with dielectric ($\varepsilon/\varepsilon_0 = 2$ in our example). In figure 2, zeroth-, first-, second-, third- and mth-order structures are shown. The number of metamaterial–vacuum interfaces is 2^m. Total length of all structures, l, is constant and the length of sections is $d = l/(N-1)$ for S_2, $S_{3+}, \ldots$ S_{N-1}, and $d/2$ for S_1 and S_N. With these dimensions and characteristic medium parameters, the perfect tunnelling conditions are satisfied, since the impedances of all inner regions (from S_1 to S_N) are matched and the optical path is zero. Field amplitudes for the zeroth (figure 2(a)) and first (figure 2(b)) -order structures are shown in figure 3, where perfect tunnelling can be observed, i.e. $|T| = 1$. From this point of view, all structures from the proposed sequence show the same behaviour. However, the field distributions along the structures are different. Figure 3 shows that there are maxima in the field amplitude in the position of each LHM–vacuum interface. The figure also shows that the value of these maxima decreases when the total number of interfaces increases. To see this fact more clearly, the field amplitudes for the first four structures of figure 2 are plotted in figure 4. Curves form a fractal object, and it is clear that the field amplitude converges to a constant value when the number of transitions tends to infinity.

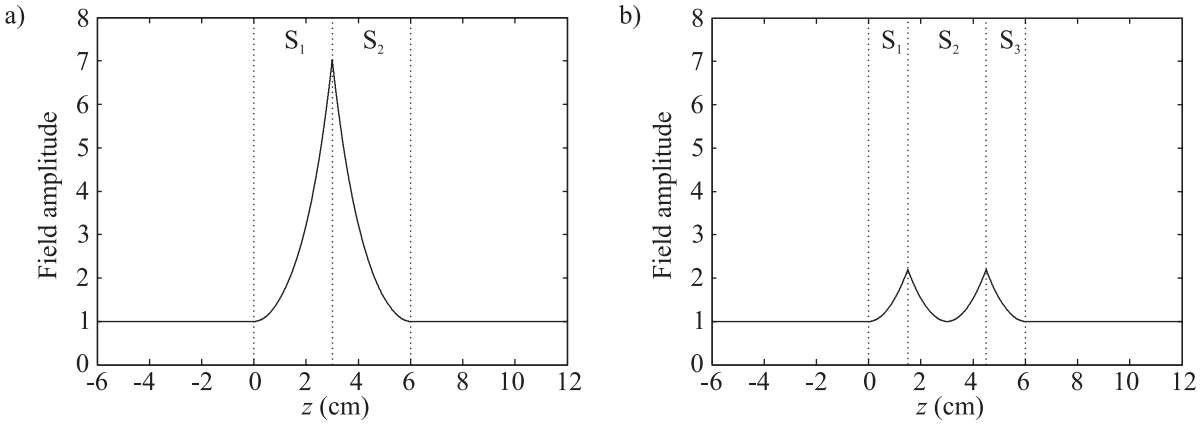

Figure 3. Field amplitude along the zeroth- and the first-order structures from figure 2. The dotted lines represent the interfaces of the structures. Width of the waveguide is $a = 2.4$ cm and operating frequency is $f = 5$ GHz. The time dependence of the field is shown in movie 1 and movie 2 respectively.

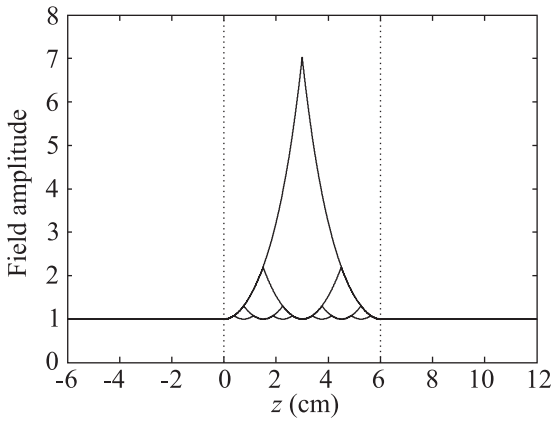

Figure 4. Field amplitude along the zeroth-, first-, second- and third-order structures. Width of the waveguide is $a = 2.4$ cm and operating frequency is $f = 5$ GHz. The values of permittivity and permeability are the same as in figure 2. The time dependence of the field is shown in movie 1, movie 2, movie 3 and movie 4 respectively.

It has been already mentioned that perfect tunnelling degrades in lossy metamaterials [10]−[12]. Since the power lost within the structure is directly proportional to the squared field amplitude, it can be concluded that losses will decay when the metamaterial is distributed in more layers [13]–[15]. Since the field amplitude converges to a nonzero value for the structure of infinite order, there exists a limit in losses different from zero. This point will be discussed in detail later. Now, analytical solution for the mth-order structure without losses will be presented, showing the convergence of the field amplitude. The field distribution within each inner region

of the mth-order structure is a linear combination of fundamental TE_{10} modes:

$$\begin{aligned} E_y &= (C_1^{\mathrm{i}} \exp[-\alpha(z - z_{\mathrm{i}})] + C_2^{\mathrm{i}} \exp[\alpha(z - z_{\mathrm{i}})]) \sin(\pi x/a), \\ H_x &= \pm(C_1^{\mathrm{i}} \exp[-\alpha(z - z_{\mathrm{i}})] - C_2^{\mathrm{i}} \exp[\alpha(z - z_{\mathrm{i}})]) \sin(\pi x/a)/Z, \end{aligned} \tag{6}$$

where $\alpha^2 = (\pi/a)^2 - (\omega/c_0)^2$ is the squared attenuation constant in each waveguide section, $Z = -\mathrm{i}\omega\mu_0/\alpha$ is the TE_{10} waveguide impedance, and $i = 1, \ldots, N$ is the index standing for each waveguide section. In the second equation of (6) plus sign is used for hollow regions and minus sign is used for regions filled with the metamaterial (with $\varepsilon/\varepsilon_0 = \mu/\mu_0 = -1$). Note that all inner waveguide sections are in cutoff, thus the attenuation constant is purely real. In the input waveguide section it can be assumed that

$$\begin{aligned} E_y &= (\exp[\mathrm{i}\beta(z - z_0)] + \mathrm{R} \exp[-\mathrm{i}\beta(z - z_0)]) \sin(\pi x/a), \\ H_x &= (\exp[\mathrm{i}\beta(z - z_0)] - \mathrm{R} \exp[-\mathrm{i}\beta(z - z_0)]) \sin(\pi x/a)/Z_0, \end{aligned} \tag{7}$$

where $\beta^2 = \omega^2\varepsilon\mu - (\pi/a)^2$ is the squared propagation constant and $Z_0 = \omega\mu_0/\beta$ is the impedance of the input and output waveguides. Similarly, the field distribution within the output waveguide is assumed to be:

$$\begin{aligned} E_y &= T \exp[\mathrm{i}\beta(z - l_N)] \sin(\pi x/a), \\ H_x &= T \exp[\mathrm{i}\beta(z - l_N)] \sin(\pi x/a)/Z_0. \end{aligned} \tag{8}$$

Coefficients in (6)–(8) are determined from the boundary conditions at the transitions. It is readily found that $C_1^{\mathrm{i}} = B\exp(-\alpha d/2)$ and $C_2^i = A\exp(\alpha d/2)$ for any metamaterial region as well as that $C_1^{\mathrm{i}} = A\exp(-\alpha d/2)$ and $C_2^{\mathrm{i}} = B\exp(\alpha d/2)$ for all vacuum regions, except of the last one, where $C_1^N = A$, $C_2^N = B$. Coefficients A and B are given by $A = T(Z + Z_0)/(2Z_0)$ and $B = T(Z_0 - Z)/(2Z_0)$. From these equalities, it follows that the transmission and reflection coefficients are $R = 0$ and $T = 1$. In the limit when the number of interfaces becomes infinite ($d \to 0$), it is clear from (6) that the field amplitude tends to the limit $E_y \to \sin(\pi x/a)$.

Two main conclusions arise from the above results. Firstly, for all structures in figure 2, all power is transmitted and there is no phase shift between the input and the output. Thus the tunnelling is 'perfect', since the incident wave is just copied from the input to the output without any reflection. Therefore the effective phase velocity in the effective medium is infinite. The second conclusion is that the field amplitude inside the in cutoff regions decreases when more metamaterial regions are introduced, and that it converges to a z-independent function when the number of regions tends to infinity. This last result can be somewhat expected from the well known fact that a periodic multilayer structure inside a waveguide behaves as an equivalent medium having an effective dielectric constant equal to the mean value of that of the layers, if their widths are small [9]. In our case, the multilayer structure can be considered as a one-dimensional realization of the 'nihility' concept previously introduced by Lakhtakia [17], which involves a medium with $\varepsilon/\varepsilon_0 = \mu/\mu_0 = 0$. It is clear that in such a medium, the phase velocity—if it has some sense—should be infinite. The attenuation constant should also be zero in such media. It is worth noting that, in spite of the fact that electromagnetic waves cannot propagate through such media [18], it has been shown that tunnelling of power is possible. This fact can be related to the aforementioned result of zero phase constant (and, therefore, zero attenuation constant too), and to the fact that the impedance in such a null medium is undetermined.

Table 1. Normalized transmitted power P_t/P_i through the structures of figure 2. Values of metamaterial characteristic parameters are $\varepsilon/\varepsilon_0 = \mu/\mu_0 = -1+\delta$. Width of the waveguide is $a = 2.4$ cm, total length is $l = 6$ cm and operating frequency is $f = 5$ GHz.

Order	Normalized transmitted power P_t/P_i					
m	$\delta = 0.001$	$\delta = 0.01$	$\delta = 0.1$	$\delta = 0.001$i	$\delta = 0.01$i	$\delta = 0.1$i
0	0.98979	0.47810	0.00527	0.86019	0.31185	0.01022
1	0.99989	0.98678	0.12531	0.97023	0.74198	0.08239
2	0.99995	0.99453	0.57084	0.98269	0.84177	0.21103
3	0.99996	0.99547	0.66355	0.98514	0.86285	0.26630
4	0.99996	0.99567	0.68333	0.98571	0.86787	0.28175
5	0.99996	0.99572	0.68806	0.98586	0.86911	0.28572
6	0.99996	0.99573	0.68923	0.98589	0.86942	0.28672

3. Losses and dispersion effects

In order to study the effects of losses and dispersion, relative permittivity and permeability of the metamaterial will be assumed in the form $\varepsilon/\varepsilon_0 = \mu/\mu_0 = -1+\delta$, where $\delta = \delta' + \mathrm{i}\delta''$ is a complex number, and $\delta'' > 0$ represents the losses in the metamaterial. Numerical values of normalized transmitted power, $P_t/P_i = |T|^2$, for several values of δ are shown in table 1 for the first six terms of the sequence of structures from figure 2. A cascade of transmission matrices similar to (3) was used to compute those transmission and reflection coefficients. From table 1 it is apparent that the transmitted power increases and converges to a constant value when the order of the structure increases. This constant value is close to one, so the transmission is quasi-perfect, for small values of δ. A similar computation has been made for the reflected power showing that reflections can also be reduced by this method. For high values of d, the impedance mismatch inside the structure becomes high. Thus, transmission is lowered and reflection is raised. For this reason the values for $\delta = 0.1$ and for $\delta = 0.1$i converge to a low value in comparison with unity.

Until now, all computations were made for normalized transversal wave number $k_t/k_0 = \lambda_0/(2a) = 1.25$. In the following, the influence of the ratio between the free-space wavelength and the waveguide width a will be investigated. When a is very small, the behaviour of input and output sections turn from propagative to evanescent. Since this fact could cause some confusion, the reference planes will be moved infinitesimally into the regions 1 and N to eliminate the matrices $\mathbf{Z}_{0,1}$ and $\mathbf{Z}_{N-1,N}$ from (3). In figure 5, similar computations to those in table 1 are shown for a wide range of k_t/k_0. Instead of transmitted power through the structure, the deviation factor $F = |1 - T|$ is depicted. Values of $F \approx 0$ mean that $|T| \approx 1$ and that the phase of T is approximately zero, i.e. that the input and output signals are approximately equal. The deviation factor is now computed for the first, second and third order of structure and it is depicted in figure 5(a) for several values of δ''. Note that the region $k_t/k_0 < 1$ means propagative waves, while $k_t/k_0 > 1$ means evanescent waves. It can be seen that there is a cutoff in the transverse wave number, such as the deviation factor is approximately one for values of k_t/k_0 higher than this cutoff. For instance, for the solid line (third-order structure) in figure 5(a), the deviation factor is smaller than 0.1 when $k_t/k_0 = \lambda_0/(2a)$ goes from zero to four, while for higher values of k_t/k_0 the deviation factor is bigger. Thus, the cutoff is approximately at $k_t/k_0 = 4$ (or $a = \lambda_0/8$). The

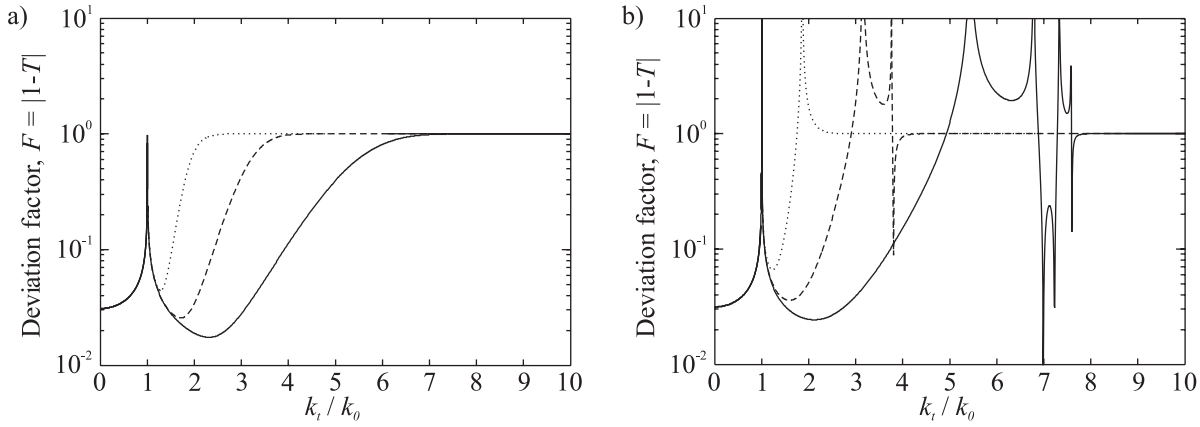

Figure 5. Deviation factor versus transversal wavevector for the first- (·····), second- (- - - - -) and third-order (——) structures. Parameters of metamaterial filled sections are: (a) $\varepsilon/\varepsilon_0 = \mu/\mu_0 = -1 + 0.01\mathrm{i}$; (b) $\varepsilon/\varepsilon_0 = \mu/\mu_0 = -0.99$.

peak at $k_t/k_0 \approx 1$ can be easily explained since, at this point, 'in cutoff' sections are close to the cutoff frequency and the overall transmission is very low. In figure 5(b), the factor F for several deviations in the real part of permittivity and permeability is depicted. Similar cutoff in the transversal wave vector is observed, but additional peaks appear which are related to excitation of surface plasmons at the interfaces.

There is a second interesting interpretation of figure 5. It is well known that the fundamental mode of a waveguide is equivalent to the superposition of two symmetrical plane waves with the same k_z and $k_t = \pm\pi/a$. This decomposition is valid even when k_z is an imaginary number, as happens in the 'in cutoff' sections. Therefore, the results in figure 5, calculated first for waveguide configurations, are applicable to the study of a multilayer metamaterial slab in free space and analysis of its focusing properties. The above-mentioned cutoff in k_t is proportional to the inverse of resolution. It is easy to see in figure 5 that the resolution of lossy and dispersive slabs is better when the number of slices is bigger, as was previously suggested in [14, 15].

4. Realistic devices with SRRs

In the text above, tunnelling enhancement was theoretically shown through a waveguide filled with isotropic left-handed material. Now, a practical realization of quasi-perfect tunnelling using anisotropic media will be analysed, and the same idea of distributing the metamaterial will be used to reduce the losses and dispersion effects. To this point assume a waveguide filled with anisotropic media with $\mu_{yy} = \mu_{zz} = \mu_0$, $\mu_{xx} < 0$ and $\varepsilon_{xx} = \varepsilon_{zz} = \varepsilon_0$, $\varepsilon_{yy} > \varepsilon_0$. It follows from Maxwell's equations that the square of attenuation constant and the wave impedance for the fundamental mode of this waveguide are given by

$$\alpha^2 = (\pi/a)^2\mu_{xx}/\mu_0 - \omega^2\varepsilon_{yy}\mu_{xx} \qquad \text{and} \qquad Z = \omega\mu_{xx}/k_z. \tag{9}$$

A complete demonstration of these expressions can be found in [20]. If $\mu_{xx} < 0$, the first equation in (9) shows that propagation of electromagnetic waves along this waveguide is only possible for $\omega < \omega_c$, where $\omega_c = \pi/(a\sqrt{\varepsilon_{yy}\mu_0})$. In contrast, if $\omega > \omega_c$ the waveguide is in cutoff and

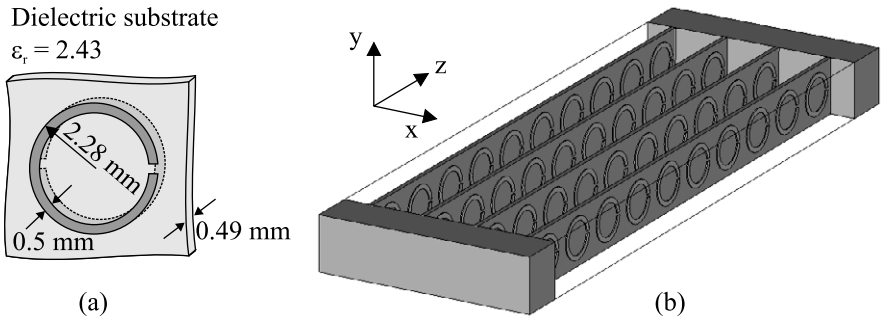

Figure 6. (a) Elementary unit of the used metamaterial is BC-SRR. (b) Waveguide fully filled with the metamaterial. Parameters are: $a = 2.4$ cm, $l = 6$ cm, unit cell $= 0.6$ cm. The input and output waveguides are filled with dielectric with $\varepsilon/\varepsilon_0 = 2.43$.

only evanescent modes can be excited. This reflects the anti-cutoff [20] properties of the medium filling the waveguide (note that the empty waveguide is in cutoff for $\omega < \omega_c^0, \omega_c^0 = \pi\, c_0/a$). If now the left-handed media in structures from figure 2 are substituted by this anisotropic metamaterial and if this medium has a dielectric permittivity $\varepsilon_{yy} > \varepsilon_0$, it is possible to find a width of the waveguide a for which the metamaterial and hollow waveguide sections are simultaneously in cutoff.

In order to obtain such kinds of anisotropic media, BC-SRR will be used as the elementary unit. Its parameters are shown in figure 6(a). The permeability of this medium is assumed in the form of the Drude–Lorenz model:

$$\mu_{xx}/\mu_0 = 1 - \delta f(2 f_0 + \delta f)/(f_0^2 - f^2), \tag{10}$$

where δf is the frequency band of negative permeability and f_0 is the resonance frequency. To estimate the parameters of the model, the setup shown in figure 6(b) was simulated using the commercial simulator *CST Microwave Studio*. The figure shows a BC-SRR loaded waveguide, sandwiched between two propagative waveguides filled with a dielectric. The calculated transmission coefficient is depicted in figure 7. Since the cutoff frequency of input and output waveguides is 4.0 GHz, the cutoff observed at 4.5 GHz belongs to the section filled with metamaterial. However, the cutoff of the hollow waveguide is at 6.3 GHz. This can be explained by introducing an effective permittivity $\varepsilon_{yy} \approx 1.93\varepsilon_0$ for the BC-SRR medium. Besides, the transmission curve shows a stop-band between 5.3 and 5.9 GHz. Inside this frequency range, $\mu_{xx} < 0$ and the waveguide is in cutoff (anti-cutoff behaviour), as can be understood from equation (9). From this last frequency band, the bandwidth is $\delta f = 0.5$ GHz and the resonance frequency is $f_0 = 5.3$ GHz. These numerical values are in agreement with others obtained experimentally in [8].

In figure 8, the BC-SRR based structures analogous to the zeroth- and the first-order structures in figure 2 are shown. The metamaterial filling the waveguide is made of an array of BC-SRRs, as is shown in figure 8. The size and periodicity of the BC-SRRs correspond to figure 7. Therefore, the values of the parameters of the medium can be assumed as they were calculated in the previous paragraph. Using these values, the ratio between the lengths of the metamaterial filled waveguide and the hollow waveguide sections, needed for achieving a 'perfect

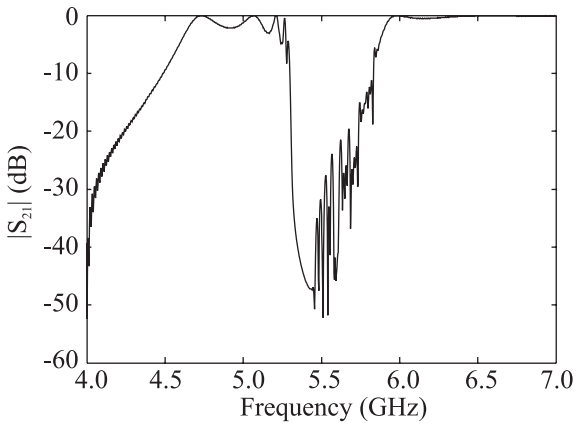

Figure 7. Magnitude of transmission coefficient for the structure sketched in figure 6.

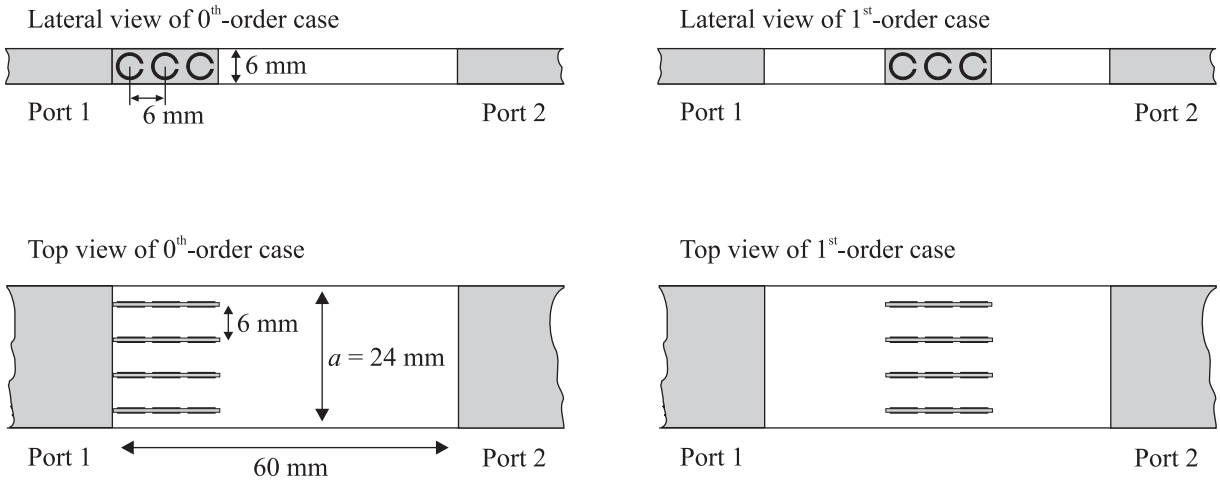

Figure 8. Structures of the zeroth and the first order.

tunnelling' of power, is determined following the method reported in [8]. Unlike in figure 2, this computation leads to a value of ∼2 for the ratio of the total lengths of the hollow waveguide sections and the metamaterial-filled sections. Thus, the aforementioned structures look as those depicted in figure 8.

The transmission coefficients for the structures shown in figure 8 have been computed by using the simulator. Theoretical results have been obtained by assuming the aforementioned continuous medium model for the BC-SRR metamaterial, and by cascading the corresponding analytical transmission matrices along the structure (just as in (3)). These results are shown in figure 9 for the lossless case, and in figure 10 for the more realistic case of lossy BC-SRRs made with copper. Clear transmission peaks appear in the frequency band of interest (from 5.3 to 5.9 GHz, where $\mu_{xx} < 0$). In the lossless case, both peaks correspond to almost 'perfect tunnelling' ($|T| = 1$), but the amplitude of these peaks is reduced when lossy metal is used (figure 10). However, this reduction is less important for the first-order structure than for the zeroth-order structure. This fact was expected because the field magnitude is lower when the

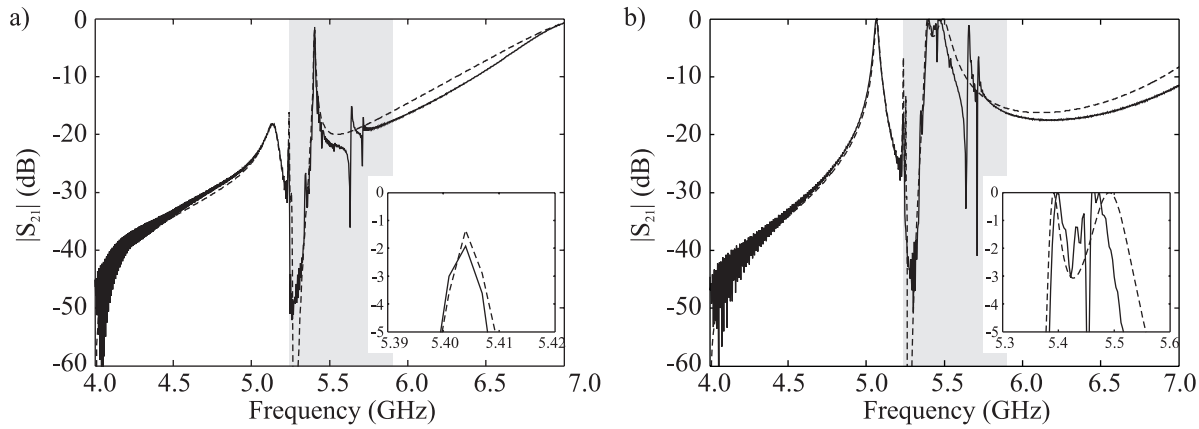

Figure 9. Magnitude of transmission coefficient for the structures sketched in figure 8 without losses. Theoretical (- - - - -) and simulation (——) results are both included. Insets show details of tunnelling peaks. (a) Results for the zeroth-order structure, (b) results for the first-order structure. The frequency band of negative permeability is indicated by a grey region.

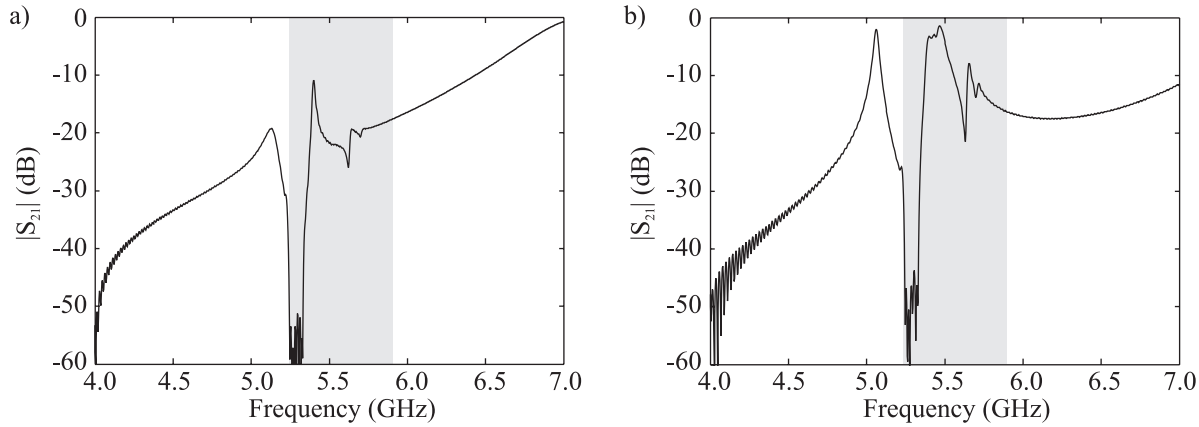

Figure 10. Magnitude of transmission coefficient for (a) zeroth- and (b) first-order structures with BC-SRRs including ohmic losses (copper was used). The frequency band of negative permeability is indicated by a grey region.

metamaterial is divided into several regions, so the dissipated energy is also lower. To check this idea, the field amplitude along the analysed structures at frequency of the aforementioned transmission peaks has been also computed using the simulator. The averaged field amplitude along the middle plane y–z of the waveguide is shown in figure 11. These results clearly show that the field amplitude is smaller in the first-order structure than in the zeroth-order one, as was predicted. Besides, the field amplitude was also calculated analytically by solving Maxwell's equations inside the waveguides, considering that the metamaterial sections were filled with the aforementioned continuous magnetic medium. The agreement between theory and simulations is actually noticeable showing the accuracy of the proposed design for the realistic implementation of multilayer 'perfect tunnelling' structures.

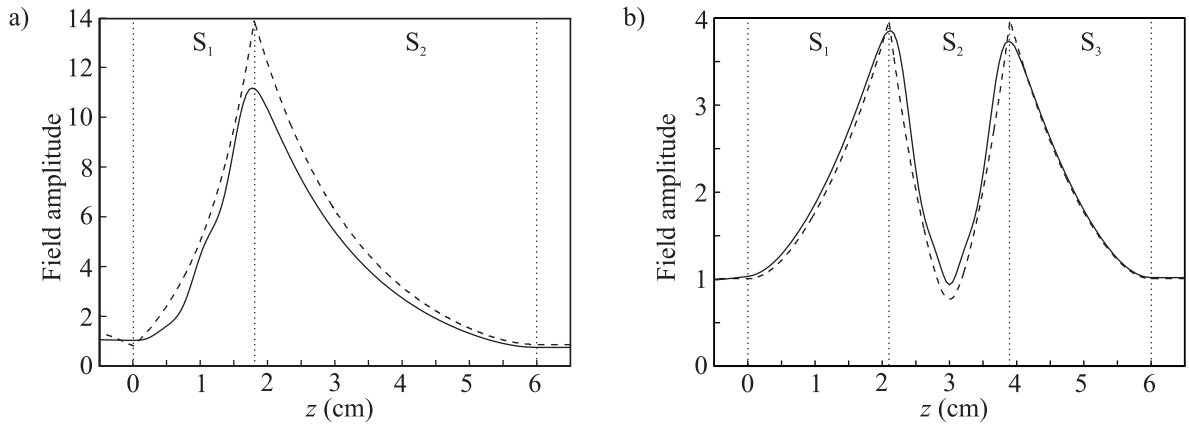

Figure 11. Field amplitude inside (a) zeroth- and (b) first-order structures without losses at 5.4 GHz, corresponding to the peaks of figure 9. Simulation (——) and theoretical (- - - - -) results are depicted.

5. Conclusion

In this paper, the behaviour of multilayer metamaterial 'perfect tunnelling' structures was analysed using a rectangular waveguide configuration. These structures have been theoretically analysed by means of a multilayer left-handed/right-handed configuration. It has been shown that the use of multiple layers leads to a significant reduction of losses and dispersion effects. The analysis also shows that there is a limit in the input/output power ratio (that corresponds to the configuration with infinite number of layers), to which this quantity converges rapidly when more layers are added to the structure (while keeping constant the total length of the tunnelling region). In the limit of infinite layers, a one-dimensional realization of the nihility concept is obtained. In this limit, the phase and the amplitude of the field are both constant along the 'in cutoff' region. This result can be put in relation with the theoretical properties of null media: zero phase and attenuation constants and indefinite impedance.

A realistic implementation of the analysed structures has been proposed. This design uses the well-known resonant and magnetic polarization properties of BC-SRRs. In this structure the isotropic LHM was substituted by anisotropic uniaxial magnetic medium, with negative magnetic permeability along its optical axis. The behaviour of the proposed configuration has been simulated by using a commercial electromagnetic solver. These simulations have shown the presence of the aforementioned effects, not only qualitatively, but also quantitatively. Thus, we feel that the reported results open the door to the realization of multilayer 'perfect tunnelling' structures made of artificial microstructured metamaterials.

Acknowledgments

This work has been supported by the Spanish Ministry of Education and Science by project contracts (TIC2001–3163, TEC2004–04249–C02–02) and by Grant Agency of Czech Republic under the project 102/03/0449. We also thank Professor J Zehetner from Czech Technical University for his kind collaboration.

References

[1] Veselago V G 1968 *Sov. Phys.—Usp* **10** 509–14
[2] Pendry J B, Holden A J, Robbins D J and Stewart W J 1999 *IEEE Trans. Microwave Theory Tech.* **47** 11
[3] Smith D R, Padilla W J, Vier D C, Nemat-Nasser S C and Schultz S 2000 *Phys. Rev. Lett.* **84** 4184–7
[4] Shelby R A, Smith D R and Schultz S 2001 *Science* **292** 77–9
[5] Pendry J B 2000 *Phys. Rev. Lett.* **85** 3966–9
[6] Grbic A and Eleftheriades G V 2004 *Phys. Rev. Lett.* **92** 117403
[7] Lagarkov A N and Kissel V N 2004 *Phys. Rev. Lett.* **92** 077401
[8] Baena J D, Jelinek L, Marqués R and Medina F 2005 *Phys. Rev.* B in press
[9] Collin R E 1991 *Field Theory of Guided Waves* 2nd edn (New York: IEEE)
[10] Garcia N and Nieto-Vesperinas M 2002 *Phys. Rev. Lett.* **88** 207403
[11] Smith D R, Schurig D, Rosenbluth M and Schultz S 2003 *Appl. Phys. Lett.* **82** 1506–8
[12] Marques R and Baena J 2004 *Microwave Opt. Tech. Lett.* **41** 290–4
[13] Shamonina E, Kalinin V A, Ringhofer K H and Solymar L 2001 *Electron. Lett.* **37** 1243–44
[14] Pendry J B and Ramakrishna S A 2003 *Physica* B **338** 329–32
[15] Ramakrishna S A, Pendry J B, Wiltshire M C K and Stewart W J 2003 *J. Mod. Opt.* **50** 1419–30
[16] Marques R, Martel J, Mesa F and Medina F 2003 *IEEE Trans. Antennas Propag.* **51** 2572–81
[17] Lakhtakia A 2002 *Int. J. Infrared Millim. Waves* **23** 339–43
[18] Lakhtakia A 2002 *Int. J. Infrared Millim. Waves* **23** 813–8
[19] Hrabar S, Bartolic J and Sipus Z 2005 *IEEE Trans. Antennas Propag.* **53** 110–9
[20] Smith D R and Schurig D 2003 *Phys. Rev. Lett.* **90** 077405